

## **N O T I C E**

THIS DOCUMENT HAS BEEN REPRODUCED FROM  
MICROFICHE. ALTHOUGH IT IS RECOGNIZED THAT  
CERTAIN PORTIONS ARE ILLEGIBLE, IT IS BEING RELEASED  
IN THE INTEREST OF MAKING AVAILABLE AS MUCH  
INFORMATION AS POSSIBLE

# Evaluation of a Method for Heat Transfer Measurements and Thermal Visualization Using a Composite of a Heater Element and Liquid Crystals

(NASA-TM-81639) EVALUATION OF A METHOD FOR  
HEAT TRANSFER MEASUREMENTS AND THERMAL  
VISUALIZATION USING A COMPOSITE OF A HEATER  
ELEMENT AND LIQUID CRYSTALS (NASA) 22 P  
HC A02/MF A01 CSCL 20D G3/34

N81-21313

Unclas  
42049

Steven A. Hippensteele, Louis M. Russell, and Francis S. Stepka  
*Lewis Research Center*  
*Cleveland, Ohio*

Prepared for the  
Twenty-sixth Annual International Gas Turbine Conference  
sponsored by the American Society of Mechanical Engineers  
Houston, Texas, March 8-12, 1981

**NASA**



EVALUATION OF A METHOD FOR HEAT TRANSFER MEASUREMENTS AND THERMAL VISUALIZATION  
USING A COMPOSITE OF A HEATER ELEMENT AND LIQUID CRYSTALS

by Steven A. Hippensteele, Louis M. Russell,  
and Francis S. Stepka

National Aeronautics and Space Administration  
Lewis Research Center  
Cleveland, Ohio

SUMMARY

Commercially available elements of a composite consisting of a plastic sheet coated with liquid crystal, another sheet with a thin layer of a conducting material (gold or carbon), and copper bus bar strips were evaluated and found to provide a simple, convenient, accurate, and low-cost measuring device for use in heat transfer research. The particular feature of the composite is its ability to obtain local heat transfer coefficients and isotherm patterns that provide visual evaluation of the thermal performances of turbine blade cooling configurations. Examples of the use of the composite are presented.

INTRODUCTION

As turbine inlet gas temperature and pressure increase, the heat loads to the turbine also increase and more complex turbine blade cooling configurations are needed to provide the desired metal temperatures and component life. The attainment of accurate metal temperature predictions and effectively cooled and durable parts requires accurate knowledge of local thermal loading in terms of the local heat transfer coefficients. The most common method used to determine these coefficients consists of finite heater strips with thermocouples (refs. 1-5). This method, however, only provides average heat transfer coefficients over a relatively large area and is generally used in one-dimensional idealizations of the problem. As a consequence methods for measuring local heat transfer are needed, particularly at near-room-temperature conditions, where the investigation can be conducted at relatively low cost and both turbine flow and heat transfer dimensionless parameters can be preserved.

This paper describes and evaluates a method that can determine local heat transfer coefficients by making use of a composite of a conductive heating element and a liquid-crystal-coated sheet. (The initial idea of a composite of these two elements was conveyed to one of the authors by Dr. Robert Moffat of Stanford University.) Liquid crystals have been used for indicating temperature change for many years (ref. 6) and have recently been used in heat transfer research by formulating and spraying liquid crystals on a test surface (ref. 7) or on a carbon-impregnated paper heater attached to a test surface (refs. 8, 9) However, these methods of applying the liquid crystals are not particularly convenient. The unique feature of the layered composite described in this paper is its simplicity, convenience of application and use, and the commercial availability of elements for fabricating the composite.

The layered composite that was evaluated at the NASA Lewis Research Center consisted of two coated plastic sheets bonded together. The first

ORIGINAL CONTAINS  
COLOR ILLUSTRATIONS

sheet, which is placed against and bonded to the test surface, has a thin layer of a conducting material (either vapor-deposited gold or coated carbon). The second plastic sheet has a thin layer of liquid crystal on its inner surface. The liquid crystal, by virtue of its color-change properties, provides a measurement of the local temperature and a visualization of thermal patterns. A heat balance and measurements of the electrical input into the conducting layer (less any heat losses) are used along with the air temperature above the layered composite and the temperature pattern indicated by the liquid-crystal sheet to provide a measure of the local heat transfer coefficient and an indication of its distribution. Inasmuch as heat losses are unique to each research application, they are not addressed in detail herein. In addition, since this study was made to illustrate examples of obtaining local heat transfer coefficient patterns rather than their absolute values, no accounting was made of the heat losses, and only minimum effort was expended in minimizing these losses.

The composite was tested in a variety of applications that included (1) a single jet of air impinging on a flat plate; (2) a large array of jets impinging on a flat plate, showing the effects of two different hole patterns; (3) the endwall of a planar turbine vane cascade with airflow through the cascade; and (4) flow out of a row of cooling air holes in a cylinder in cross-flow, which simulates a film-cooled turbine vane leading edge. Also investigated were the accuracy and uniformity of heat distribution in the heater element, temperatures indicated by the liquid-crystal sheet, and thermal patterns in the composite. The paper describes the composite in detail and its accuracy and uniformity and shows photographs of the thermal patterns obtained. Dr. Russell H. Kulas of the College of Wooster evaluated the vapor-deposited gold heater material.

#### SYMBOLS

A	area
d	derivative
h	heat transfer coefficient
q	heat flux (or electric power input)
r	electrical resistance
t	temperature
1,2	conditions

#### Subscripts:

a	air
c	liquid crystal at calibrated color
e	electric power input

losses

Superscript:

(-) average

## DESCRIPTION OF COMPOSITE ELEMENTS

### Liquid-Crystal Sheet

There are three types of liquid crystals: smectic, nematic, and cholesteric. The molecular structure of the liquid crystal determines the particular type. The cholesteric type was used in this study. The unique property of cholesteric liquid crystals is their ability to reflect definite colors at specific temperatures for a given material. Cholesteric substances mixed in various proportions can produce many different temperature-color combinations. The color change for the liquid crystal that was used in this study ranges from clear at ambient temperature (before melting starts) through red as the temperature increases and then to yellow, green, blue, and finally clear again at the highest temperature (after melting completely). These color changes are repeatable and reversible as long as the liquid crystals are not physically damaged by excessive temperature. More information about the theory of liquid crystals can be obtained from reference 6.

The liquid-crystal material used in this study was purchased commercially as sheets that consisted of the liquid crystals laid on a black plastic sealing material and covered by a transparent Mylar layer. The overall thickness of the sheet was 0.203 mm (0.008 in.), and it was available in 0.305-m (1-ft) widths of any length.

### Heater Element

The heater element consisted of either a thin, vapor-deposited coating of gold on a polyester film or a carbon-impregnated coating on a plastic sheet. Both were purchased commercially. The overall thicknesses of the sheets with their coating were 0.127 mm (0.005 in.) and 0.178 mm (0.007 in.), respectively. The sheets with the gold deposit were 0.914 m (3 ft) wide and could be purchased in any length. The carbon-coated sheets were 43.2 cm (17 in.) wide and could be purchased in lengths of 55.9 cm (22 in.).

### Composite

The composite of the liquid crystal and the heater sheet, made up of commercially available materials, is shown in cross section in figure 1. The lower layer of the composite was the heater sheet. The copper bus bars were attached to the conductive side (top) along two opposing outer edges of the sheet. Although the copper strips had conductive adhesive backing, this adhesive alone did not produce adequate or consistent electrical contact. A silver-impregnated paint was therefore used to bridge a portion of the copper strip and conductive material, as shown in the figure. The upper layer of the composite was the liquid-crystal sheet. The liquid-crystal sheet was attached to the lower layer (heater sheet) by an adhesive, with the bus bars sandwiched between. Electric wires were connected to the bus bars by standard soldering

methods. The overall thickness of the composite was approximately 0.508 mm (0.020 in.).

The composite sheet can be attached to the test surface by any adhesive that would give smooth, uniform contact over the surface. In this study, a thin, paper-like material with double adhesive backing was used both for attaching the composite to the test surface and for attaching the liquid-crystal sheet and the heater sheet together.

## EVALUATION

### Apparatus and Procedure

Liquid-crystal sheet. The liquid-crystal sheets were calibrated for color versus temperature by immersing the sheet in a hot water bath and observing and photographing (with strobe lights) the color changes as the water gradually cooled to room temperature. The water bath was stirred before temperature measurements and photographs were taken. The sheet had been enclosed in a watertight plastic bag before immersion to protect it from any possible detrimental effects of the water. The water temperature was measured by a copper-constantan thermocouple and a precision digital voltmeter.

Heater element. Two types of heater elements were examined: vapor-deposited gold on a polyester film and a conductive, carbon coating on a plastic sheet. The accuracy of the heat transfer coefficient depends on the uniformity of heating in the heater element portion of the composite. Heating uniformity was therefore measured. To determine heating uniformity in the vapor-deposited gold sheets, two methods were used: measuring the uniformity of light transmission, and measuring the voltage at regular intervals over the surface. Only the voltage-measuring method, using a digital multimeter, was used for the carbon-coated sheets. It was reasoned that the uniformity of the gold sheet for heating was related to the uniformity of the gold thickness and in turn to the uniformity of the light transmission through the gold, or the light density. The light density was measured by using a video image processor and a scanning microdensitometer.

Composite. After separate evaluations were made of the liquid-crystal sheet and the two types of heater element sheets, selected liquid-crystal sheets laminated to the heater sheets were evaluated as composites. Copper bus bars were attached to opposite edges of the heater sheets as described previously (fig. 1). A conventional power supply and digital multimeters were used to measure the amounts of electric power passing into the heater sheets. The composite sheets were suspended horizontally in a cardboard frame surrounded by plastic walls to provide a dead air space that would minimize the free-convection heat transfer. Knowing the uniformity of the liquid-crystal sheets and that of the heater sheets evaluated earlier, we could now assess the uniformity of the composite by passing electric power into it. The resulting liquid-crystal temperature pattern was recorded with a 35-mm camera by using color film and strobe lights as in the water calibration discussed previously.

Although the effects of free convection (ref. 10) on creating nonuniform heat transfer were initially of concern, simple tests were run to allay this concern. Regions of nonuniformity due to the heater element were the same even with the sheet in a vertical position, where the effect of free convection is known to be greater and is evident and superimposed on the nonuniform

pattern. Also, heating the composite in the horizontal position by means of a radiant heat source gave color uniformity, an indication that no significant nonuniformity was caused by free convection. As a consequence any nonuniformities observed in the composite were due to the nonuniformity of the composite elements and not to any free-convection effects.

Determination of the heating uniformity of the composites requires the use of an air energy balance for the surface-convection heat transfer

$$q_e - q_f = hA(t_c - t_a) \quad (1)$$

where  $q_e$  is the measured electric power (or heat transfer rate) input to the composite heater,  $q_f$  is the sum of all heat transfer rate losses from the composite heater except the surface-convection heat loss,  $h$  is the surface-convection heat transfer coefficient,  $A$  is the composite area heated,  $t_c$  is the calibrated temperature of the specific color used, and  $t_a$  is the temperature of the air above the composite surface. The  $q_f$  term includes heat conduction losses through the composite walls and heat radiation losses from the composite to the surroundings. Because the heater element is very thin, losses due to lateral heat conduction are considered negligible.

Specifically, to determine the heating uniformity of any area in a composite sheet requires two measurements: the  $q_{e,1}$ , required to produce the first sign of the calibrated color being used, and the  $q_{e,2}$ , required to produce the last sign of this same calibrated color. The first measurement shows the localized hottest spot and the second shows the coldest spot. These measurements must be done while the surrounding air temperature and velocity remain constant and only after equilibrium conditions have been reached. The localized spots found during these measurements each have the same calibrated color and therefore the same temperature  $t_c$ . At these localized spots the heat fluxes  $dq_1/dA$  are the same because the temperatures of the spots  $t_c$  and of their surroundings  $t_a$  are the same. Also, at these spots the free-convection heat transfer coefficients  $h$  can be considered to be the same. Now, if energy balance equation (1) is written for each of the two measured conditions, and if the two equations are subtracted from each other, then

$$dq_{e,2} - dq_{e,1} = (h_2 - h_1) (t_c - t_a) dA \quad (2)$$

Therefore the localized electric power (or heat flux) at the two spots must be identical since the difference in the identical-valued heat transfer coefficients is zero.

The pattern of the localized resistance of the heater element material remains the same within any given composite sheet if the resistance change of the heater element material with temperature is considered negligible. This is the case over the range of temperatures found in the composite during testing. A calculation of the resistance variation in the gold heater sheet, which was worse than that of the carbon sheet, showed that it varied by less than 1 percent over the range of temperature encountered. The localized electric power (or heat flux) at any spot  $dq_e/dA$  is directly related (linearly) to the resistance at that spot  $dr$  for a given current through, or voltage across, that spot. The total electric power or heat flux for the total sheet  $q_e/A$  is directly related (linearly) to the average resistance of the sheet  $\bar{r}$  for a given current through, or voltage across, the sheet. At any specific spot the relative error in the localized resistance  $dr$  (expressed as a

percentage deviation from the average resistance in that sheet  $\bar{r}$ ) remains constant because the localized resistance values remain the same. Therefore, since heat flux is directly related (linearly) to resistance, the localized heat flux error (expressed as a percentage deviation from the total heat flux for the sheet) is directly related to the differences in the total heat flux values. The maximum percentage error in a given composite of the localized heat flux was obtained from the expression

$$\left[ \frac{q_{e,2} - q_{e,1}}{(q_{e,2} + q_{e,1})/2} \right] \times 100 \quad (3)$$

## Results and Discussion

Liquid-crystal sheet. The results of a typical temperature color calibration for a particular liquid-crystal sheet done in the water bath are shown in figure 2. The data covered a range of temperatures from 52.1° C (125.8° F) to 36.1° C (96.9° F). As shown in the figure the colors that corresponded to the hottest to coldest temperatures included blue, green, yellow, and red. At 38.1° C (100.5° F), or green, the sheet had only a slight amount of yellow. At 37.6° C (99.7° F), or yellow, it had only a slight amount of red. Therefore the yellow color occurred very uniformly over the entire liquid-crystal sheet and represented an extremely narrow temperature band. For this reason the yellow color was used to determine the 37.6° C (99.7° F) temperature isotherm in this particular liquid-crystal sheet. The yellow color appears between the dominant red and green colors and is estimated to define an isotherm temperature to within 0.2 degree C (0.4 deg F). Others (refs. 11, 12) claim that by special selection of the types of liquid crystals an accuracy of 0.1 degree C (0.2 deg F) can be achieved. The ANSI type T (copper-constantan) thermocouple material used here has a maximum error in absolute temperature indication of 0.42 degree C (0.75 deg F). However, when the same thermocouple and microvoltmeter are used to measure the difference between the water calibration temperature and the air temperature during testing, only a negligible error exists. This sheet was used in the first three tests made to illustrate the uses of the composite. Water bath calibrations were done for other liquid-crystal sheets, and each specific color resulting from a particular water bath temperature was very uniform throughout the sheet. However, the specific colors did vary for given temperatures from sheet to sheet. It is therefore necessary to calibrate each particular sheet when using it to obtain quantitative heat transfer data. Also, the viewing angle for the liquid crystal in research use should not be much different than that when calibrating the material. The reason for this is that a shift in the color band positions (temperature indication) occurs with changes in the viewing angle to the liquid-crystal sheet surface. This shift, however, was only significant when the viewing angle changed from the surface-normal by more than about 30°.

In summary, the liquid-crystal sheets evaluated herein responded very uniformly to temperature over their entire area. Using the calibrated, highly temperature-sensitive yellow color provides an accurate means of determining a detailed temperature isotherm to within 0.2 degree C (0.4 deg F).

Heater element. The video image processor was used to measure the photographic density of the vapor-deposited gold sheet, or the light transmitted through the gold layer. The photographic density variations in the gold were



smaller than the detection capability of the video system even with considerable computer processing.

Next the scanning microdensitometer was used to produce maps of isodensity contours of the vapor-deposited gold. The edges of the roll of the heater material were found to have rather severe density gradients that would result in nonuniform current and heat flow. The microdensitometer could not detect the density variations occurring over very small distances such as apparent cracks or kinks resulting from handling. Also, prescreening of the gold film sheets using this scanning microdensitometer is not practical for general use because only a 20- by 10-cm (7.9- by 3.9-in.) region can be scanned at once, and each scan requires about 90 minutes plus setup time. The method, however, did provide information on the uniformity of the conductive material.

The measurement and mapping of the equipotential contours for both the gold-coated sheet and the carbon-coated material indicated that they are parallel and equidistant except for very local disturbances such as the microscopic cracks or kinks just mentioned. This indicates that the current flow in the film is in parallel lines between the bus bars. The resistivities of the gold-coated sheet and the carbon-coated material were also measured and found to be 3.3 and 50.0 ohms per square, respectively.

The tests discussed so far in this section provide information on the relative uniformity of the conductive materials. A more appropriate method of evaluating the heater element is described next. In this method the combination of the heater element and the liquid-crystal sheet is tested. Because the liquid-crystal sheet is very uniform and accurate, any nonuniformity shown in the liquid-crystal sheet while it is in the composite is a direct result of the nonuniformity of the heat flux in the heater sheet.

Composite. Two composites containing liquid-crystal sheets that had a yellow color calibration temperature of  $31.7^{\circ}\text{C}$  ( $89.0^{\circ}\text{F}$ ) were made and evaluated. The first composite also contained a 30.5- by 61.0-cm (12- by 24-in.) portion of a gold sheet randomly chosen from the 91.4-cm (36-in.) wide roll material. The second composite also contained a randomly chosen 21.6- by 27.9-cm (8.5- by 11.0-in.) carbon-coated heater sheet. Because the liquid-crystal sheets respond very uniformly to the calibrated temperature (yellow color), any nonuniform yellow color (nonuniform temperature pattern) is a direct indication of nonuniformity in the heat flux from the heater sheet.

The first composite (fig. 3) was used to show, quantitatively, the nonuniformity in the heat flux (or heat transfer coefficient) due to the nonuniformity of the gold film in the heater sheet. The bus bars were located along the top and bottom edges. The nonuniformities in this composite are located inside the dashed lines. This area, which is 41.7 cm (16.4 in.) long by 28.2 cm (11.1 in.) wide, excludes the extreme nonuniformities along each end of the composite. Note that the light spots in the lower right corner are strobe light reflections. The first measurement, showing the localized hot spots, is shown in figure 3(a). The second measurement, showing the localized cold spots, is shown in figure 3(b). The respective heat transfer rates are 39.2 and 46.0 w. From these data and equation (3) the maximum percentage error in the localized heat flux within this specified area was determined to be  $\pm 8$  percent. This is the same error that could be expected in the heat transfer coefficient within this specified area. By making more measurements in between these two, localized spots can be calibrated, and therefore localized heat fluxes or heat transfer coefficients can be corrected. Also, the areas

of these large sheets that have more uniform heat fluxes and thereby produce more accurate heat transfer coefficients can be selected.

The second composite, containing the carbon-coated heater element, was briefly evaluated, but no photographs were taken. The uniformity of its heat flux, as revealed by the resulting liquid-crystal isotherm colors, was as good as that of the gold-coated heater sheet material. Handling problems (producing kinks or cracks) were not observed. Even purposely made surface scratches did not produce any noticeable localized temperature nonuniformities. Based on the preliminary findings the carbon-coated material appears to be as good as, or maybe better than, the gold-coated material for use as the heater element.

In summary, the tests of the composites indicate that localized heat flux or measurement of heat transfer coefficients can be determined to about  $\pm 8$  percent or even less if careful selection is made of the heater sheet.

#### RECOMMENDED PROCEDURE FOR USE

The following procedure must be followed when quantitative heat transfer data are desired. The specific liquid-crystal sheet used must be water calibrated to determine the temperature of the yellow color isotherm. The most uniform heater sheet area must be chosen by making up different composites and observing the heat flux nonuniformities (isotherms). This should be done while electric power is applied to the heater sheet and the composite is suspended horizontally in a dead air space. Once a sheet is selected, additional measurements of the nonuniform heat flux may be needed in order to calibrate the localized areas of the sheet, as discussed earlier in this paper. These additional measurements will allow the correction of the localized heat transfer coefficient because the yellow pattern, being an isotherm, does not necessarily represent an iso-heat-transfer coefficient.

As shown in equation (1) the heat losses must be accounted for. When the selected composite sheet is installed in the test facility, preliminary calibration measurements must be made just before testing if quantitative heat transfer data are to be obtained. The sum of the heat losses can be determined by measuring the electric power input to the heater element that is required to bring the liquid-crystal temperature up to the calibrated yellow color. At the yellow isotherms these heat losses will be the same as during the tests because the temperatures will be the same. This is to be done before any airflow (e.g., impingement, film cooling, passage, etc.) is provided to the test model. Of course, as with any quantitative heat transfer study the use of guard heaters and insulation and the establishment of equilibrium conditions are necessary. Because of the variation in thermocouple material, it is best to use the same thermocouple in the test as was used in the water calibration of the liquid-crystal sheet. In this way the error in the thermocouple will be cancelled out when the temperature difference is taken between the water calibration temperature of the yellow isotherm and the air temperature during the test. From the measured sum of the heat flux losses, the heated area of the sheet, and the additional electric power input to obtain the yellow color for the research flow environment, the local heat transfer coefficient is determined by using equation (1). It is this additional electric power input (heat flux) that is being transferred from the sheet to the environment to compensate for the heat transfer coefficient present during the test.

## ILLUSTRATIONS OF USE

### Apparatus and Procedure

The apparatus for illustrating the use of the liquid-crystal and heater element composite for several heat transfer applications where knowledge of local heat transfer coefficients is needed is shown in figures 4 to 6.

The general procedure for conducting the tests was to first flow current through the heater sheet until color change started to occur in the liquid-crystal sheet. The composite and the test apparatus were allowed to reach thermal equilibrium with occasional slight changes in the current flow. Next, the tunnel gas flows and coolant flows were set to the desired values. Then the electric current through the heater sheet was changed to provide the desired temperature patterns. After equilibrium conditions were reached, the input electrical heat flux was measured and still photographs of the thermal patterns were taken with a 35-mm camera. The illumination was provided by two conventional strobe lights.

Impingement cooling. The apparatus that was used to illustrate how the composite can be used to obtain local heat transfer coefficient patterns for an impingement-cooled wall is shown schematically in figure 4. The apparatus consisted of a transparent plastic (acrylic) test section that permitted visual observation and photography of the color pattern in the liquid-crystal sheet. Ambient room-temperature air was first drawn into the upper enclosed plenum and then through a perforated transparent plate to impinge on a movable (impingement) plate to which the liquid-crystal and heater element composite was attached. The air then exited into the tunnel ducting and into the laboratory vacuum exhaust system. Tests were run with plates that were perforated with (1) a single hole, (2) an array of eight rows of holes with an in-line hole pattern, and (3) an array of eight rows of holes with a staggered hole pattern. The perforated plate was 1.27 cm (0.5 in.) thick, 38.1 cm (15 in.) wide, and 61.0 cm (24 in.) long. All holes were 1.27 cm (0.50 in.) in diameter. The plate with the single hole was spaced a distance of six hole diameters from the impingement plate. The airflow rate through the hole was set to give a flow Reynolds number of 5000 based on hole diameter. These conditions were set to be within the applicable range of the heat transfer coefficient correlation of reference 13 so that an approximate comparison of results could be made. For the plates with eight rows of holes, the lateral hole spacing was four hole diameters and the spacing in the tunnel flow direction was five hole diameters. The distance from the perforated plate to the impingement plate was two hole diameters. The airflow rate for these plates was set to also give a flow Reynolds number of 5000. The geometry and flow conditions for these plates were set to be within the experimental range of the data in reference 4 so that approximate comparison could be made with the results of reference 4, which showed that the in-line hole array would provide better cooling than the staggered array.

The liquid-crystal and heater element composite was attached to the top side of the impingement plate in the manner described in the section DESCRIPTION OF COMPOSITE ELEMENTS. The bus bars for the heater sheet for this application were attached at the edges of the heater sheet and parallel to the airflow direction, as shown in figure 4. The dimensions of the composite sheet were 16.5 cm (6.5 in.) by 25.4 cm (10 in.). The previously described general procedure was then followed.

Endwall of a cascade. The plastic tunnel and cascade that were used for illustrating how the liquid-crystal and heater element composite can be used to obtain local heat transfer coefficient patterns for the endwalls of a cascade are shown schematically in figure 5. The cascade had an axial chord of 11.4 cm (4.5 in.), a ratio of pitch to axial chord of 1.08, and an aspect ratio (span to axial chord) of 1.34.

The cascade test section, with the location of the composite sheet, is shown in figure 5(b). The liquid-crystal side of the composite sheet with dimensions of 16.5 cm (6.5 in.) by 25.4 cm (10 in.) was attached to the inside of the ceiling of the cascade. In this installation the bus bar strips were attached to the edges of the heater sheet that were approximately perpendicular to the flow direction. Paper cutouts of the vane cross sections were attached to the top of the plastic tunnel directly over the respective location of the vanes for visual orientation. For these tests ambient room-temperature air was drawn through the tunnel to flow through the cascade and over the composite attached to the endwall. Airflow velocity through the cascade was set to give a flow Reynolds number (based on actual chord) of  $1.475 \times 10^5$  in order to approximate the range of experimental results from flow visualization experiments at the endwall of this cascade reported in reference 14. The air then exited through the laboratory vacuum exhaust system. The previously described general procedure was then followed.

Film injection from a cylinder. The schematic of the transparent plastic tunnel shown in figure 6(a) was used to illustrate how the liquid-crystal and heater element composite can be used to obtain local heat transfer coefficient patterns resulting from air injection from a cylinder in crossflow. Ambient room-temperature air was drawn into the tunnel, flowed over the cylinder, and then exited through the laboratory vacuum exhaust system. A separate air supply from the laboratory service air system was ducted into the test cylinder to flow out a row of two holes in the surface that simulated film cooling holes at the leading-edge region of a turbine vane. Main-stream flow Reynolds number (based on cylinder diameter) was set at a value of  $1.2 \times 10^5$  to correspond to the conditions in reference 15, in which results of a smoke visualization of the flow out of this cylinder are described.

The test section, the cylinder, and the injection flow tubes are shown schematically in figure 6(b). The test cylinder was a hollow, black, opaque plastic tube that was 11.4 cm (4.5 in.) in diameter and 15.2 cm (6.0 in.) high. The inside of the test cylinder had two tubes with an inside diameter of 1.09 cm (0.43 in.) at an angle of  $30^\circ$  to the vertical for supplying the injection air. These tubes terminated flush with the surface of the test cylinder. For these tests the vertical centerline through the two holes was located at an angular distance of  $30^\circ$  from the stagnation point.

The cylinder with the liquid-crystal and heater element composite attached to it is shown in figure 6(c). For reasons of expediency and availability of composite sheet material, one edge of the sheet was located along the centerline of the row of holes. The edge of the composite near the holes was faired to avoid tripping of the flow. For these tests the bus bar strips were parallel to the tunnel wall and were wrapped around the periphery of the cylinder. The previously described general procedure was then followed.

## Results and Discussion

Impingement cooling. The thermal pattern on the liquid-crystal sheet at a typical test condition of the impingement of a single jet onto a flat plate is shown in figure 7. The figure shows the concentric patterns representing isotherms or regions of constant heat transfer coefficients generated by the impacting jet (assuming uniform heat flux from the heater element). The color changes starting at the center are black, dark red, red, yellow, green, blue, and black. The yellow color, representing a temperature of  $37.6^{\circ}\text{C}$  ( $99.7^{\circ}\text{F}$ ), gave the most distinctive change and was considered as the one that could best be used for quantitatively determining the local heat transfer coefficient, as described in the section EVALUATION.

By increasing the electric power input into the composite at a constant-airflow condition, the convective heat pickup was increased. Equation (1) shows that this heat pick-up is the difference between the electric power input and the losses. Since the air temperature and the reference temperature of the wall (as indicated by the yellow color in the liquid-crystal sheet) are constant, the magnitude of the local heat transfer coefficient  $h$  (as indicated by yellow) also increases with electric power input. Although the measurements made with the single jet were not intended to provide absolute values of the local  $h$  pattern, approximate values showed a trend of decreasing  $h$  with increasing radii similar to that obtained in reference 13.

The resulting isotherm and constant heat transfer coefficient patterns for the in-line and staggered impingement hole arrays are shown in figure 8. The photographs, which were taken of the fifth to eighth rows downstream, show how the accumulation of upstream flow progressively influences the deflection of the thermal pattern in the downstream direction. The results for both arrays show the distinct influence of the impingement from each hole. As a result the local heat transfer coefficient varies across the wall. In an application of impingement cooling this variation of heat input could cause variations in local temperature and induce thermal gradients that could affect the life of the part.

The relative cooling effectiveness of the two arrays is indicated by the relative extent of the dark areas inside the yellow isotherm. These are areas of high heat transfer coefficients. Comparison of the two arrays shows that for the same condition of flow the in-line hole array has larger areas of higher coefficients and therefore is more effectively cooled than the staggered array configuration. The photograph also shows that the relative cooling effectiveness for both configurations increased with downstream distance. These results agree with those of reference 4, which were obtained from one-dimensional measurements of the heat transfer coefficients in the streamwise direction by means of copper heater strips.

Although tests conducted herein were not intended to obtain absolute values of the heat transfer coefficient, the results showed agreement of the relative performance of cooling effectiveness with another experiment. Also these tests provided information on the local and lateral variation of the coefficient that could not be obtained by the one-dimensional measurement method used in reference 4.

Endwall of a cascade. The isotherm and local heat transfer coefficient patterns for the endwall of a cascade are shown in figure 9. The photograph shows that the region of high heat transfer at the endwall surrounds the airfoil. This is the region bounded by the yellow color. The heat transfer co-

efficient was higher nearer the airfoil, as indicated by the color change from red to black. The photograph also shows that the region of high heat transfer at the wall is larger in extent near the pressure surface than near the suction surface. These results support the flow visualization that was conducted with this cascade (ref. 14), which showed that a leading-edge-generated vortex near the endwall moved away from the leading-edge pressure surface as it traveled downstream. This vortex apparently reduced the boundary layer on the wall near the pressure side as it progressed downstream, resulting in the higher heat transfer coefficient indicated in reference 16.

Film injection from a cylinder. The isotherm and heat transfer coefficient pattern obtained by the injection of air from a row of two holes in a cylinder in crossflow are shown in figure 10. The holes were located at an angle of  $30^\circ$  from the stagnation point. This test simulated the flow of cooling air from film cooling holes at the leading edge of a turbine vane. Although the holes in the cylinder were inclined at an angle of  $30^\circ$  from the vertical, the main stream dominated the flow direction of the injected flow. This is shown in figure 10 by the isotherms downstream of the hole, which show only a slight deviation from the mainstream direction. The figure also shows that the influence of the injected air on cooling is also constrained to a narrow region downstream of the hole with only little spreading. These results support those in reference 15 obtained by visualization of the flow out of this cylinder.

#### CONCLUDING REMARKS

The composite of liquid crystal and heater element investigated herein, when used in a test installation in which proper accounting is made for conduction and radiation losses, provides a relatively convenient, simple, inexpensive, and accurate device for the high-resolution measurement of heat transfer and for determining local heat transfer coefficients at near-room-temperature conditions for a variety of applications. This investigation, which evaluated the accuracy and feasibility of commercially available elements of the composite, provided the basis for using the composite for quantitative heat transfer experiments. The liquid-crystal sheet of the composite was found to indicate a temperature to within 0.2 degree C (0.4 deg F) at the calibrated yellow color of  $37.6^\circ\text{C}$  ( $99.7^\circ\text{F}$ ). Other sheets have color change temperatures up to  $250^\circ\text{C}$  ( $482^\circ\text{F}$ ) but with limited sensitivities. The electrically generated heat flux out of the heater element was found to vary within 8 percent for a specified area of large heater sheets. Consideration of these accuracies indicated that if the composite elements can be selected within a specified area, and if conduction and radiation losses to other parts of the test installation are properly accounted for, the local heat transfer coefficient error can be held to values even smaller than 8 percent.

Although the method was used herein primarily to illustrate qualitatively the results expected from application of the composite, the results confirmed inferences from flow visualization and heat transfer results of others in addition to providing information on local heat transfer that was not available in those experiments.

In conclusion the method can be used for both comparisons of relative heat transfer performance of geometric configurations and quantitative local heat transfer determination. Some of the applications for the method in addition to the four examined qualitatively herein include various configurations

of airfoils, coolant passages in multipass blade designs, curved ducts of different aspect ratios, and other three-dimensional geometries.

#### REFERENCES

- 1 Eriksen, V. L., "Summary Report on Film Cooling Effectiveness and Heat Transfer with Injection Through Holes," NASA CR-72991, 1971.
- 2 Choe, H., Kays, W. M., and Moffat, R. J., "Turbulent Boundary Layer on a Full-Coverage Film-Cooled Surface - An Experimental Heat Transfer Study with Normal Injection," NASA CR-2642, 1976.
- 3 Luckey, D. W., and L'Ecuyer, M. R., "Stagnation Region Gas Film Cooling - Spanwise Angled Cooled Injection." TSPC-TR-76-2, Dec. 1976, Purdue University, Lafayette, Ind. (AD-A035716)
- 4 Florschuetz, L. W., Metzger, D. E., Takeuchi, D. I., and Berry, R. A., "Multiple Jet Impingement Heat Transfer Characteristic - Experimental Investigation of Inline and Staggered Arrays with Crossflow," ERC-R-79034, Jan. 1980, Arizona State University, Tempe, Ariz. (NASA CR-3217.)
- 5 VanFossen, Jr., G. J., "Heat Transfer Coefficients for Staggered Arrays of Short Pin Fins," For presentation at the 1981 ASME Gas Turbine Conference, Houston, Texas, March 8-12, 1981. (NASA TM-81596.)
- 6 Ferguson, J. L., "Liquid Crystals," Scientific American, Vol. 211, No. 2, Aug. 1964, pp. 76-85.
- 7 den Ouden, C., and Hoogendoorn, C. J., "Local Convective-Heat-Transfer Coefficients for Jets Impinging on a Plate - Experiments Using a Liquid-Crystal Technique." Proceedings of the Fifth International Heat Transfer Conference, Vol. V, AIChE, New York, 1974, pp. 293-297.
- 8 Cooper, T. E., Field, R. J., and Meyer, J. F., "Liquid Crystal Thermography and Its Application to the Study of Convective Heat Transfer," Journal of Heat Transfer, Vol. 97, Aug. 1975, pp. 442-450.
- 9 do Carmo Durao, M., "Investigation of Heat Transfer in Straight and Curved Rectangular Ducts Using Liquid Crystal Thermography." M.S. Thesis, Naval Postgraduate School, Monterey, Calif., June 1977. (AD-A045131)
- 10 Velarde, M. G., and Normand, C., "Convection," Scientific American, Vol. 243, No. 1, July 1980, pp. 92-108.
- 11 Butefisch, K. A., "The Liquid Crystal Method for the Visualization and Measurement of Heat Transfer Distributions," Methods for Heat Transfer Measurement, DLR-Mitt 75-11, Feb. 1976, European Space Agency, Paris, pp. 48-68.

12 McComas, J. P., "Experimental Investigation of Ground Effects on a Heated Cylinder in Crossflow," M.S. Thesis, Naval Postgraduate School, Monterey, Calif., Dec. 1974. (AD/A-004240.)

13 Walz, D. R., "Spot Cooling and Heating of Surfaces with High Velocity Impinging Air Jets, Part 2 - Circular Jets on Plane and Curved Surfaces." TR 61, July 1964, Stanford University, Calif. (AD-607727.)

14 Gaugler, R. E., and Russell, L. M., "Streakline Flow Visualization Study of a Horseshoe Vortex in a Large-Scale, Two-Dimensional Turbine Stator Cascade," ASME Paper No. 80-GT-4, Mar. 1980.

15 Russell, L. M., "Flow Visualization of Discrete Hole Film Cooling with Spanwise Injection over a Cylinder," NASA TP-1491, 1979.

16 Graziani, R. A., et al., "An Experimental Study of Endwall and Airfoil Surface Heat Transfer in a Large Scale Turbine Blade Cascade," ASME Paper No. 79-GT-99, Mar. 1979.



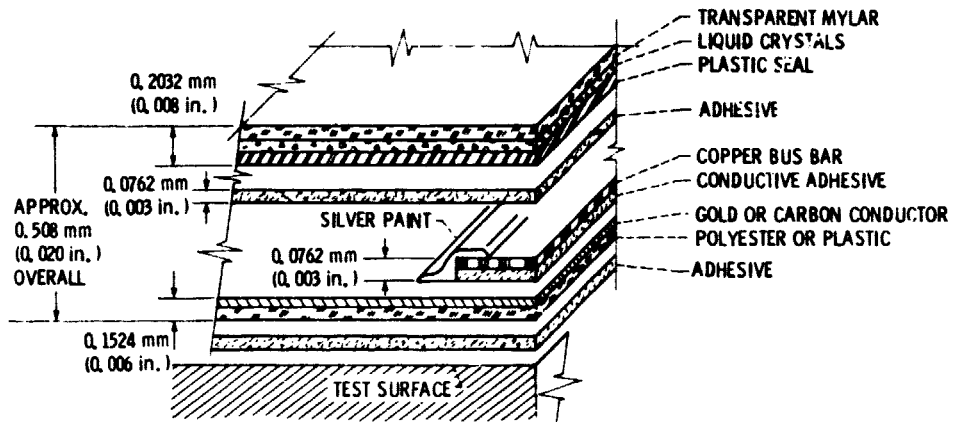


Figure 1. - Liquid-crystal sheet - electric heater composite (not to scale).

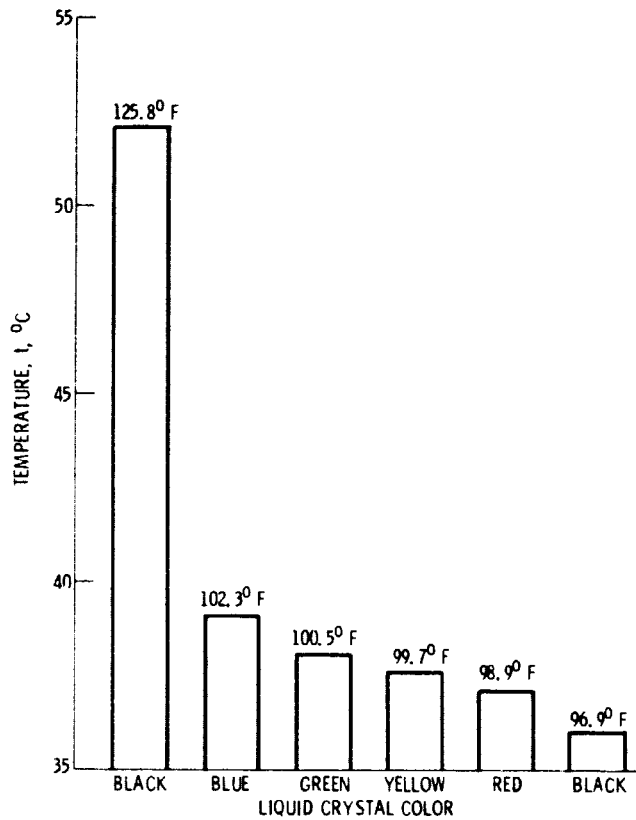
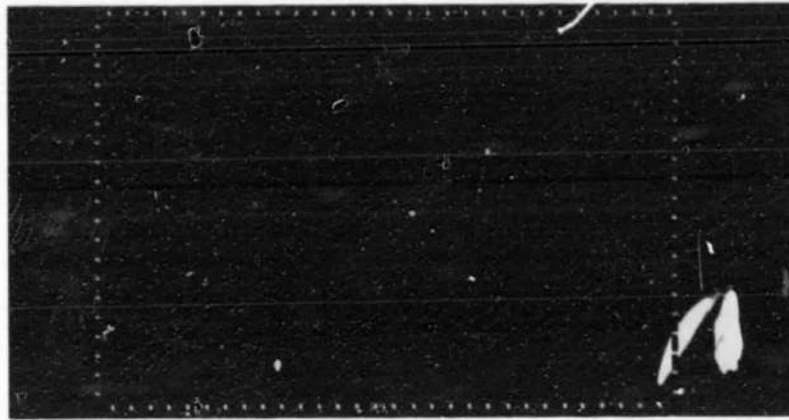
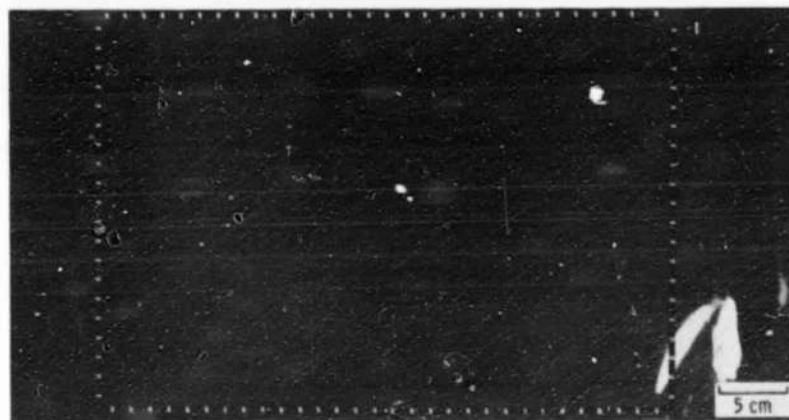


Figure 2. - Calibration of liquid crystal color with temperature.



(a) YELLOW BEGINNING.



(b) YELLOW ENDING

Figure 3. - Uniformity test of the gold heater sheet and liquid-crystal sheet with electric power supplied.

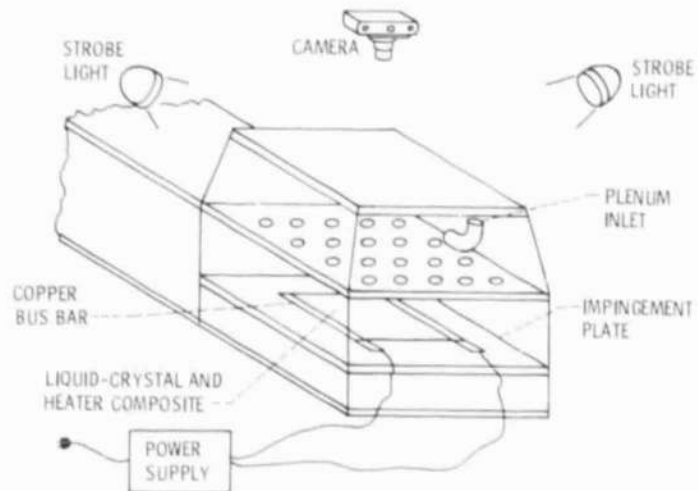
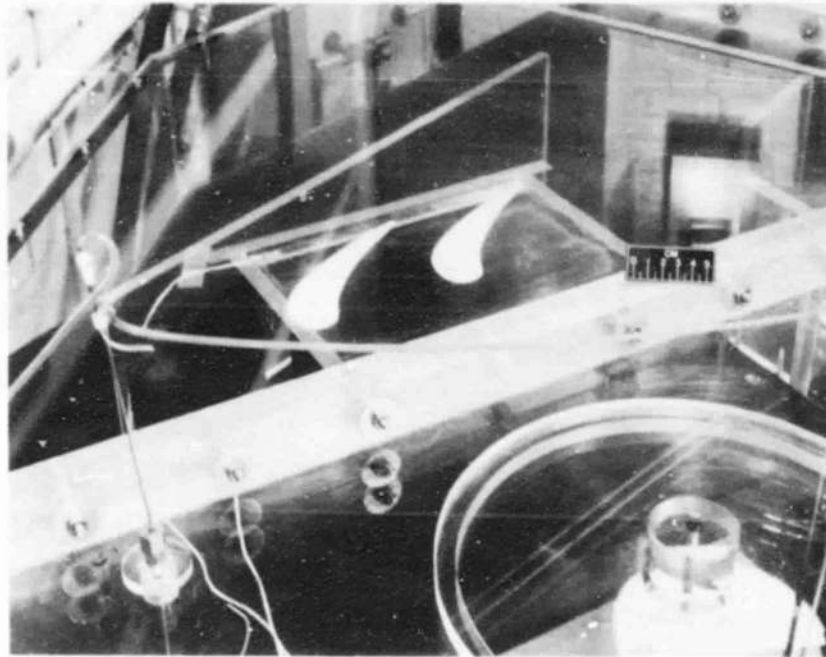
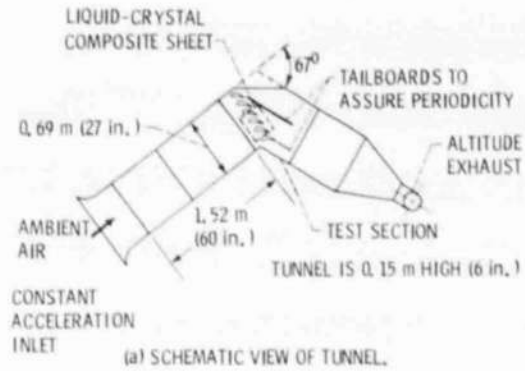


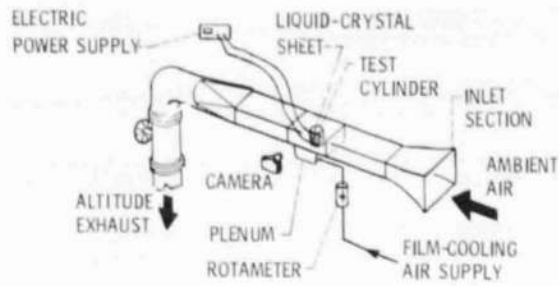
Figure 4. - Impingement cooling thermal visualization apparatus.



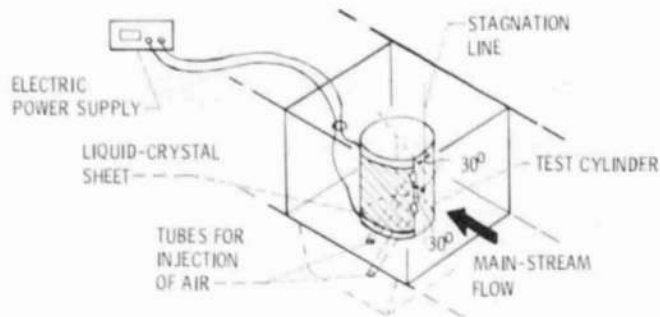
(b) CASCADE ENDWALL TEST SECTION.

Figure 5. - Cascade endwall thermal visualization apparatus.

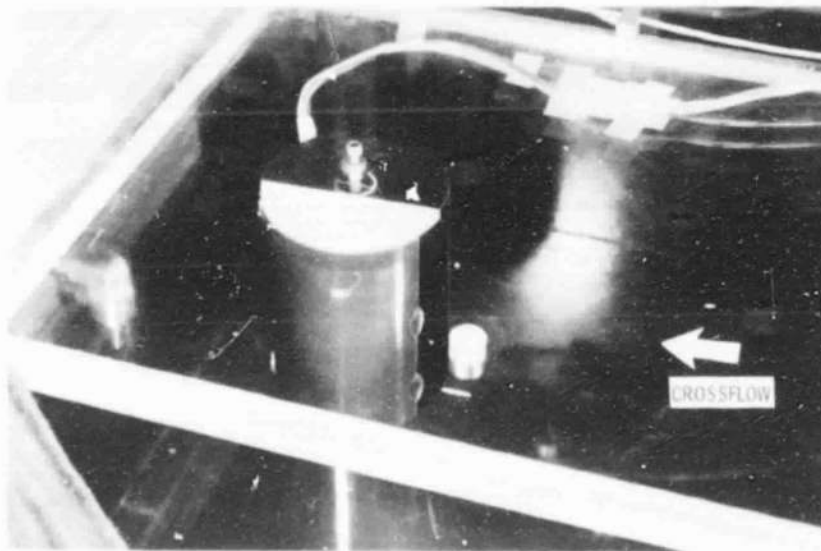
ORIGINAL PAGE IS  
OF POOR QUALITY



(a) SCHEMATIC OF TUNNEL.



(b) TEST SECTION, WHERE THE INJECTION ANGLE RELATIVE TO THE CYLINDER SURFACE AND THE ANGULAR LOCATION FROM THE STAGNATION LINE ARE BOTH  $30^\circ$ .



(c) TEST CYLINDER.

Figure 6. - Film injection from a cylinder in crossflow, thermal visualization apparatus.

ORIGINAL PAGE IS  
OF POOR QUALITY

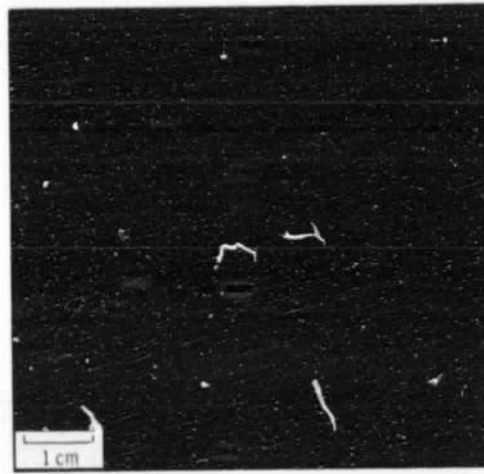
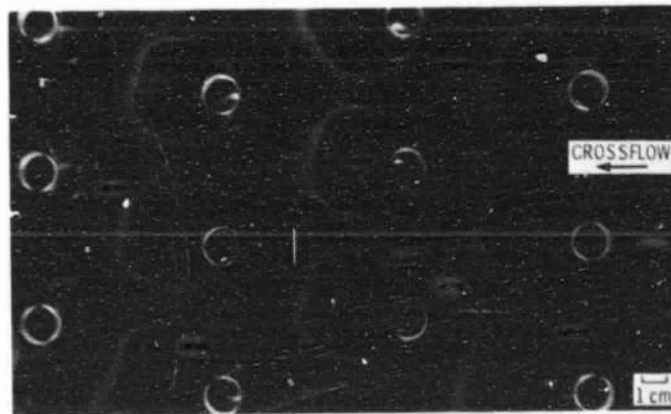
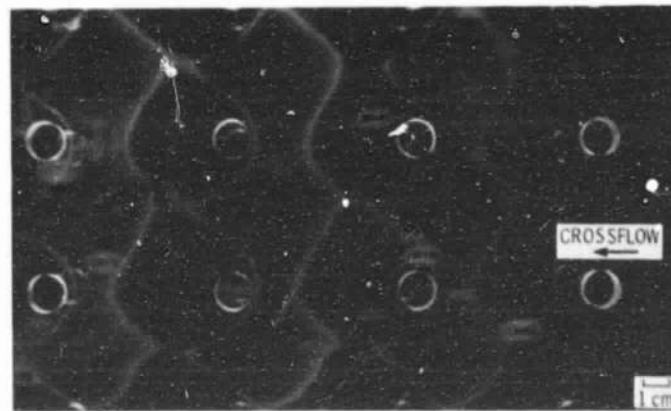


Figure 7. - Single-hole jet impinging on a flat plate.



(a) STAGGERED ARRAY.



(b) INLINE ARRAY.

Figure 8. - Impingement cooling, downstream rows 5 to 8.

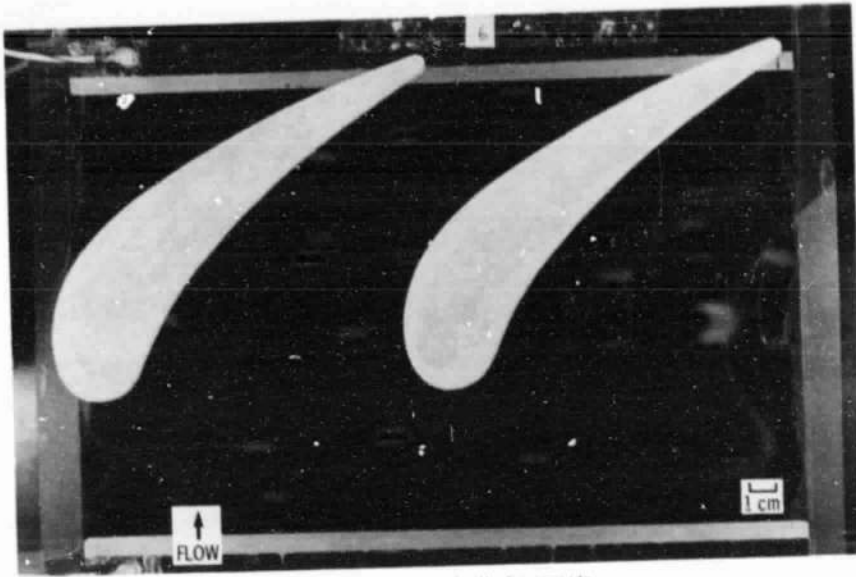


Figure 9. - Vane endwall of a cascade.

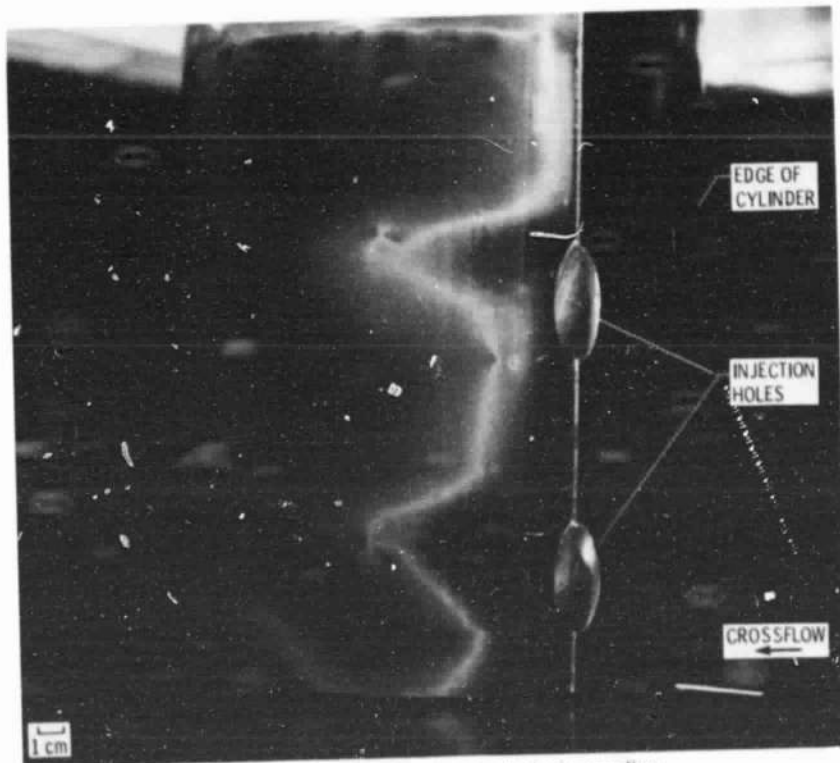


Figure 10. - Film injection from a cylinder in crossflow.